

Original paper

# Phosphate minerals from the hydrothermal quartz veins in specialized S-type granites, Gemerská Poloma (Western Carpathians, Slovakia)

Martin ŠTEVKO<sup>1\*</sup>, Pavel UHER<sup>1</sup>, Jiří SEJKORA<sup>2</sup>, Radana MALÍKOVÁ<sup>2,3</sup>, Radek ŠKODA<sup>3</sup>, Tomáš VACULOVIC<sup>4</sup>

<sup>1</sup> Department of Mineralogy and Petrology, Faculty of Natural Sciences, Comenius University, Ilkovičova 6, 842 15 Bratislava, Slovak Republic; stevko@fns.uniba.sk

<sup>2</sup> Department of Mineralogy and Petrology, National Museum, Cirkusová 1740, 193 00 Praha 9-Horní Počernice, Czech Republic

<sup>3</sup> Department of Geological Sciences, Faculty of Science, Masaryk University, Kotlářská 2, 611 37 Brno, Czech Republic

<sup>4</sup> Department of Chemistry, Faculty of Science, Masaryk University, Kamenice 5, 625 00 Brno, Czech Republic

\*Corresponding author



An interesting association of phosphate minerals (fluorapatite, triplite, arrojadite-group minerals and viitaniemiite) was studied from intra-granitic hydrothermal quartz veins with minor amounts of albite, orthoclase, muscovite, fluorite, rhodochrosite, arsenopyrite, pyrite, bismuthinite and kobellite. The veins occur in highly evolved, Permian topaz-zinnwaldite leucogranite at the Elisabeth adit near Gemerská Poloma, Gemic Unit, Western Carpathians (eastern Slovakia). Fluorapatite is enriched in Mn (~4 wt. % MnO, 0.3 *apfu* Mn) and frequently replaced by triplite, representing the first known triplite occurrence in Western Carpathians. This mineral forms irregular aggregates ( $\leq 7$  cm across), Mn/(Mn + Fe) atomic ratio of which attains 0.68 to 0.78 and F/(F + OH) = 0.89–0.92. “Fluorarrojadite-(BaNa)” to its Mn-dominant analogue “fluordickinsonite-(BaNa)” (both minerals still not approved by IMA-CNMNC) occurs as aggregates up to 2 cm across, showing Sr-rich (~1.7 wt. % SrO, ~0.36 *apfu* Sr) and Sr-poor ( $\leq 0.6$  wt. % SrO,  $\leq 0.13$  *apfu* Sr) compositions with *W* site F/(F + OH) = 0.74–0.80 and *M* site Mn/(Mn + Fe) = 0.39–0.52. Rare viitaniemiite is Mn-rich (10 to 11 wt. % MnO, 0.34–0.38 *apfu* Mn). The phosphate mineralization in quartz represents a high-temperature hydrothermal assemblage. The F-rich Mn, Fe, Ca-bearing phosphates, fluorite, and muscovite precipitated most likely in presence of alkali- and fluorine-bearing post-magmatic fluids which altered primary magmatic minerals (especially Li-rich micas and alkali feldspars) and liberated some elements (Fe, Mn, Al, Ba, Sr, Na, K) from the adjacent granite.

**Keywords:** hydrothermal phosphates, triplite, arrojadite group, chemical composition, S-type granite, Slovak Republic

Received: 24 July, 2015; accepted: 9 December, 2015; handling editor: I. Broska

## 1. Introduction

Phosphate minerals represent widespread minor to accessory constituents of various magmatic to hydrothermal systems, especially in highly fractionated, P-rich peraluminous granite-pegmatite suites and greisenized granites, commonly with orogenic and post-orogenic S-type affinity (e.g., London 1997; Breiter et al. 1997, 2005; Piccoli and Candela 2002; Sejkora et al. 2006; Petrik et al. 2011; Baijot et al. 2012; Llorens and Moro 2012; Roda-Robles et al. 2012). Textural relationships, internal zoning and compositional variations of principal phosphate minerals (mainly apatite-group minerals, amblygonite, triphyllite-lithiophyllite, triplite-zwieselite, and other Fe-Mn phosphates) represent sensitive indicators of magmatic to hydrothermal evolution in such systems. Specific P-T-X-fO<sub>2</sub> conditions lead to precipitation of unique chemical compositions of some phosphate minerals, for example in the arrojadite-group minerals (Chopin et al.

2006). Therefore, detailed knowledge of the nature and chemistry of phosphate minerals is an important tool for our understanding of magmatic to hydrothermal processes and role of phosphorus in highly evolved silicic rocks (London 1992, 1997; Breiter et al. 1997, 2005).

In the present work, we describe phosphate mineral association (fluorapatite, triplite, arrojadite-group minerals and viitaniemiite) from intra-granitic hydrothermal quartz veins in the highly fractionated topaz-zinnwaldite leucogranites at the Elisabeth adit near Gemerská Poloma, eastern Slovakia. The paper documents presence of rare phosphate minerals: “fluorarrojadite-(BaNa)” together with its Mn-dominant analogue “fluordickinsonite-(BaNa)” (both are phases not yet approved by IMA-CNMNC) and viitaniemiite. Similar minerals have been recently described in the nearby Surovec Li-F granite by Petrik et al. (2011). Still, the phosphate mineralization at Gemerská Poloma represents the first reported occurrence of triplite in the Western Carpathians.

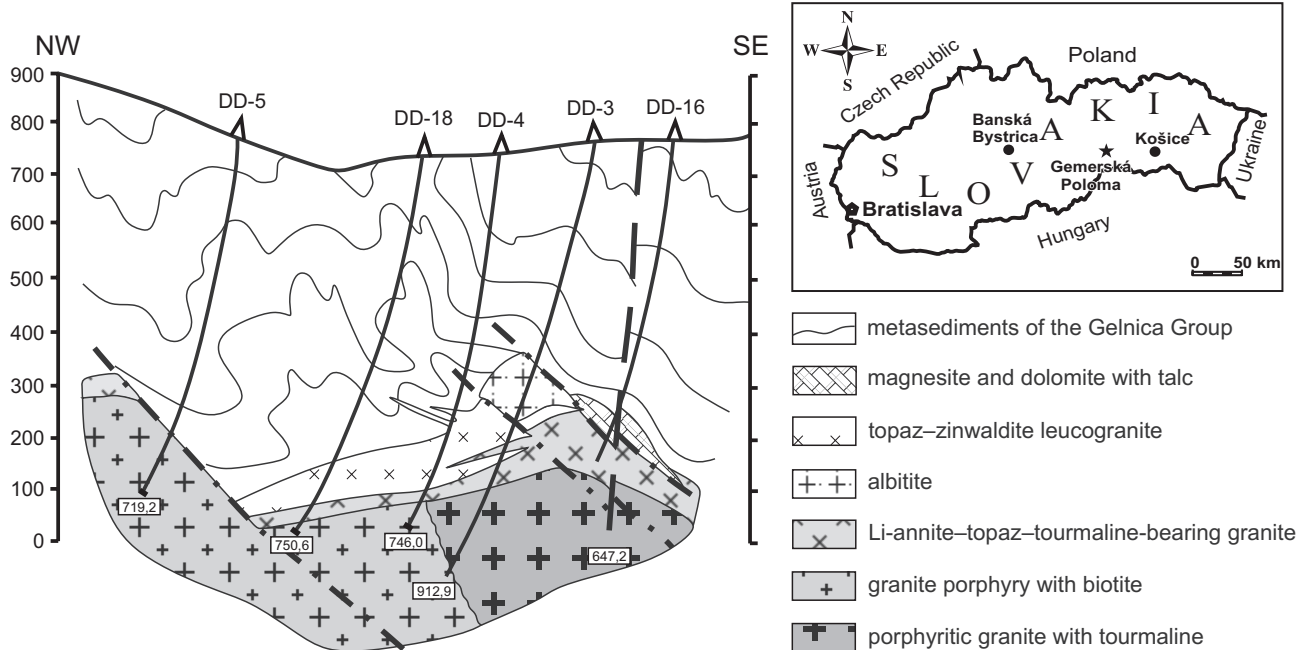


Fig. 1 Location and NW–SE cross section of the granite pluton near Gemerská Poloma (modified after Dianiška et al. 2002).

## 2. Geological setting

The hydrothermal quartz veins are developed in the specialized Gemic granites, which were recently located during the driving of Elisabeth adit at the Gemerská Poloma talc deposit, located about 10 km north-west of Rožňava, Gemic Unit, Slovak Republic [GPS 48°45'4.07"N and 20°29'39.32"E].

The granitic rocks of the Gemic Unit represent a distinct type of specialized (Sn–W–F), highly evolved suite with S-type affinity that differs from other granitoids occurring in the Veporic and Tatic Units of the Western Carpathian crystalline basement. Besides fluorine, they are enriched in phosphorus and rare lithophile elements, such as Li, Rb, Cs, B, Ga, Sn, W, Nb, Ta, U and depleted in REE, Zr, Ti, Sr, Ba (e.g., Uher and Broska 1996; Petrík and Kohút 1997; Kubiš and Broska 2005, 2010). Recent zircon U–Pb and molybdenite Re–Os isotopic dating indicate emplacement of the Gemic granites and related post-magmatic mineralization during Late Permian (~260 to 230 Ma; Poller et al. 2002; Kohút and Stein 2005; Gaab et al. 2006). Younger, Alpine (Cretaceous) fluid-driven low-temperature tectono-metamorphic overprint affected the granitic rocks along mylonite zones (Breiter et al. 2015).

The Gemic granitic rocks form several small plutons that intruded the intensively folded Lower Paleozoic (mainly Ordovician to Devonian) volcano-sedimentary complex of the Gelnica Group, metamorphosed under greenschist-facies metamorphic conditions (Bajaník et al. 1984; Petrasová et al. 2007). In the investigated Gemerská Poloma area, the metamorphic rocks are

composed mainly of phyllites, metapyroclastic rocks of rhyolitic to dacitic composition, locally with lenses of metadolomite and strongly stearitized magnesite. The latter have been recently exploited as a talc deposit near Gemerská Poloma (Kilík 1997). Several types of granites were distinguished in the studied area (Fig. 1): (1) coarse-grained porphyritic granite to granite porphyry, (2) medium-grained Li-annite-topaz-tourmaline bearing granite, (3) P-enriched topaz-zinnwaldite leucogranite and (4) albitite (Dianiška et al. 2002, 2007; Petrík et al. 2014; Breiter et al. 2015).

Except for albitites, all listed granitoid types were found in the Elisabeth adit. Hydrothermal quartz veins with albite, muscovite, fluorite, carbonates, sulfides and sulfosalts were observed in all types of granite, but the occurrence of quartz veins with phosphate mineralization is limited only to the topaz-zinnwaldite leucogranite. The veins with phosphates are up to 8 cm thick and more than 3 m long and in addition to phosphates they also contain minor amounts of albite, orthoclase, muscovite, fluorite, carbonates (Mn-rich siderite, rhodochrosite and dolomite), arsenopyrite, pyrite, bismuthinite and kobellite.

Tab. 1 Refined unit-cell parameters of triplite from Gemerská Poloma in comparison with published data

	this work	Waldrop (1969)	Downs (2006)
$a$ [Å]	12.085(7)	12.065(1)	12.036(2)
$b$ [Å]	6.463(5)	6.454(1)	6.4646(3)
$c$ [Å]	9.941(6)	9.937(1)	9.965(1)
$\beta$ [°]	107.09(4)	107.093(6)	106.75(1)
$V$ [Å <sup>3</sup> ]	742.1(6)	739.59	742.5(1)

\* Fe and Mg-rich triplite

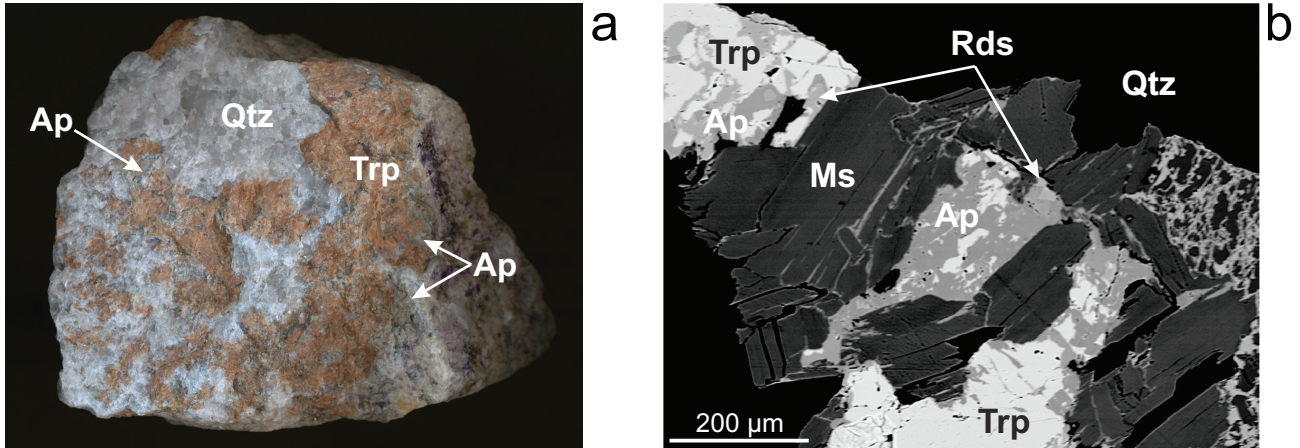


**Fig. 2** Triplite from Gemerská Poloma. **a** – Brown-red subhedral to anhedral grains and aggregates of triplite (Trp) replacing green-grey fluorapatite (Ap) enclosed in quartz (Qtz), width of image: 20 cm; **b** – Homogenous aggregates of triplite (Trp) replacing fluorapatite (Ap) associated with muscovite (Ms) and minor rhodochrosite (Rds), BSE image.

### 3. Analytical methods

The morphology of minerals was studied with the Olympus SZ-61 optical microscope in combination with the Olympus SP-350 digital camera (Department of Mineralogy and Petrology, Faculty of Natural Sciences, Comenius University in Bratislava, Slovakia), used for photography in incandescent light.

The powder X-ray diffraction (P-XRD) data for phosphates were obtained on a Bruker D8 Advance diffractometer equipped with solid-state LynxEye detector and secondary monochromator producing  $\text{Cu}K_{\alpha}$  radiation housed at the same institution. The instrument was operating at 40 kV and 40 mA. In order to minimize the background, the powder samples were placed on the surface of a flat silicon wafer in ethanol suspension. Positions and intensities of diffractions were processed using a pseudo-Voigt shape function with the High-Score Plus (PANalytical) program. Unit-cell parameters were refined by least-square method with the Celref program (Laugier and Bochu 2011). For the arrojadite group minerals, unit-cell parameters were refined using structural data published by Chopin et al. (2006) for fluorarrojadite–(BaFe).

Quantitative chemical analyses of phosphates were carried out using a Cameca SX100 electron microprobe (Laboratory of Electron Microscopy and Microanalysis of the Masaryk

University and Czech Geological Survey in Brno, Czech Republic) in the wavelength-dispersion mode. Operating conditions were 15 kV, 10–20 nA and a 5–10  $\mu\text{m}$  beam diameter. The following lines and standards were used: fluorapatite (P, Ca  $K_{\alpha}$ ), GaAs (As  $L_{\alpha}$ ), spessartine (Si, Mn  $K_{\alpha}$ ), titanite (Ti  $K_{\alpha}$ ), sanidine (Al, K  $K_{\alpha}$ ), gahnite (Zn  $K_{\alpha}$ ), almandine (Fe  $K_{\alpha}$ ),  $\text{Mg}_2\text{SiO}_4$  (Mg  $K_{\alpha}$ ),  $\text{SrSO}_4$  (Sr  $L_{\alpha}$ ), barite (Ba  $L\beta$ ), albite (Na  $K_{\alpha}$ ), topaz (F  $K_{\alpha}$ ), and

**Tab. 2** Chemical composition of triplite from Gemerská Poloma (in wt. %)

Anal. #	117	118	119	129	130	131
$\text{P}_2\text{O}_5$	32.30	32.42	32.83	32.83	32.61	32.75
FeO	19.71	19.41	17.62	13.70	13.62	14.80
MnO	42.30	40.74	44.58	48.39	49.01	47.03
MgO	0.46	0.44	0.44	0.34	0.33	0.32
CaO	1.40	1.64	1.08	1.04	0.99	1.11
$\text{H}_2\text{O}$ calc.	0.38	0.44	0.35	0.38	0.36	0.41
F	7.82	7.72	8.04	7.86	7.97	7.91
Cl	0.03	0.06	0.00	0.00	0.00	0.00
O=F	-3.29	-3.25	-3.39	-3.31	-3.36	-3.33
O=Cl	-0.01	-0.01	0.00	0.00	0.00	0.00
Total	101.10	99.61	101.55	100.78	101.53	101.00
P <sup>5+</sup>	1.000	1.000	1.000	1.000	1.000	1.000
Fe <sup>2+</sup>	0.603	0.591	0.530	0.418	0.413	0.446
Mn <sup>2+</sup>	1.310	1.257	1.359	1.495	1.504	1.437
Mg <sup>2+</sup>	0.025	0.024	0.024	0.018	0.018	0.017
Ca <sup>2+</sup>	0.055	0.064	0.042	0.041	0.038	0.043
Sum A	1.993	1.936	1.955	1.972	1.973	1.943
OH <sup>-</sup>	0.094	0.107	0.085	0.093	0.087	0.098
F <sup>-</sup>	0.904	0.890	0.915	0.907	0.913	0.902
Cl <sup>-</sup>	0.002	0.004	0.000	0.000	0.000	0.000
Sum X	1.000	1.001	1.000	1.000	1.000	1.000
O <sup>2-</sup>	3.993	3.936	3.954	3.972	3.972	3.943
Sum cat.	2.993	2.936	2.955	2.972	2.973	2.943
Sum an.	4.993	4.937	4.954	4.972	4.972	4.943
Mn/(Mn+Fe)	0.68	0.68	0.72	0.78	0.78	0.76

Formulae based on P = 1 apfu and (OH+F+Cl) = 1 apfu

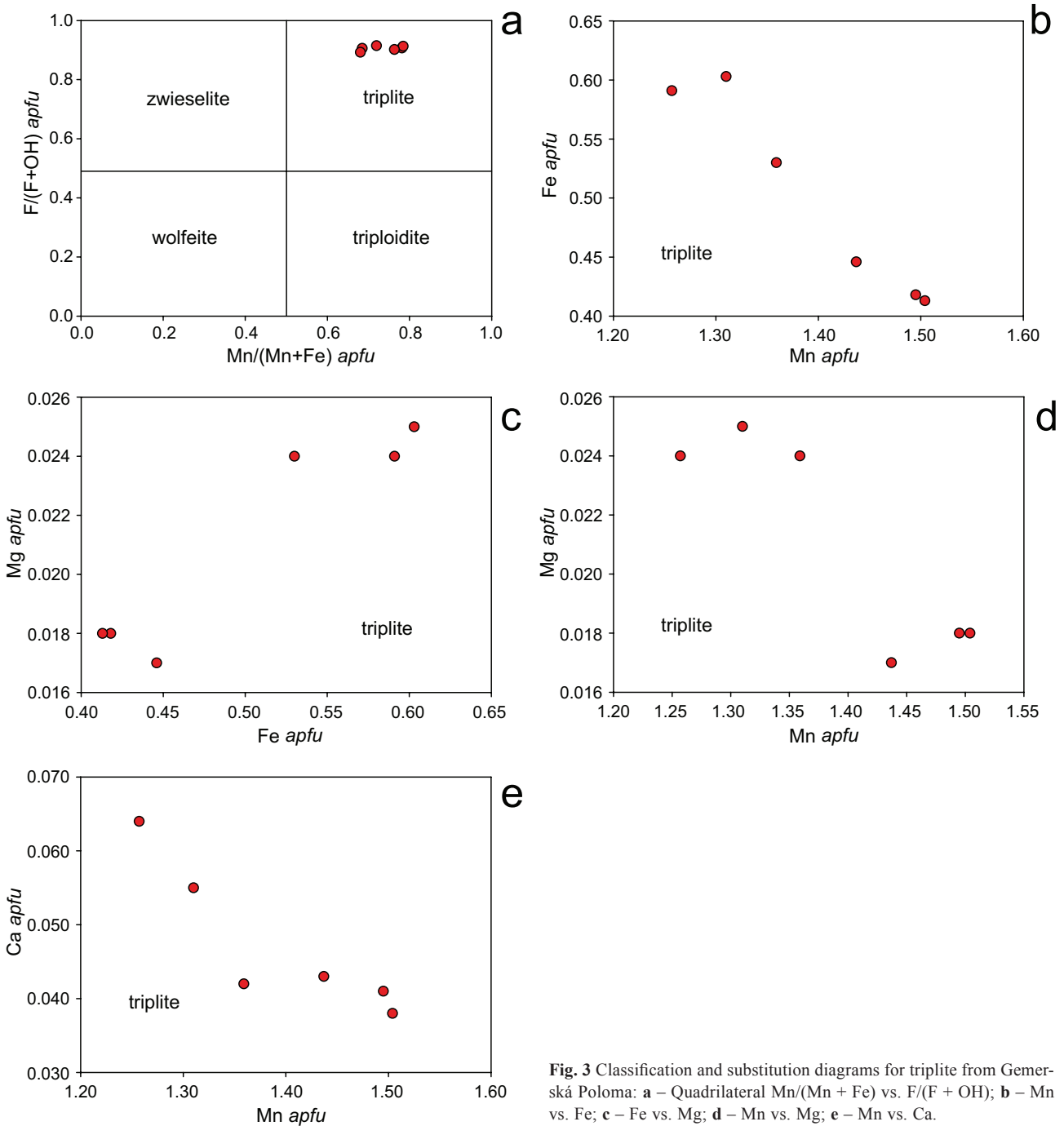


**Fig. 3** Classification and substitution diagrams for triplite from Gemerská Poloma: **a** – Quadrilateral  $\text{Mn}/(\text{Mn} + \text{Fe})$  vs.  $\text{F}/(\text{F} + \text{OH})$ ; **b** –  $\text{Mn}$  vs.  $\text{Fe}$ ; **c** –  $\text{Fe}$  vs.  $\text{Mg}$ ; **d** –  $\text{Mn}$  vs.  $\text{Mg}$ ; **e** –  $\text{Mn}$  vs.  $\text{Ca}$ .

vanadinite ( $\text{Cl K}_a$ ). Raw intensities were converted to the concentrations using automatic PAP matrix correction (Pouchou and Pichoir 1985).

Major- and trace-element concentrations in phosphate samples were determined by LA-ICP-MS at the Department of Chemistry, Faculty of Science, Masaryk University, Brno (Czech Republic). The setup consists of laser-ablation system UP213 (New Wave, USA) and quadrupole ICP-MS Agilent 7500ce (Agilent Technologies, Japan). Ablation system is equipped with Nd:YAG

laser emitting radiation with wavelength of 213 nm. The sample is placed in ablation cell (Supercell®, New Wave, USA) where the interaction of laser radiation with sample occurs. The ablated material is transported by carrier gas (helium) with flow rate of 1.0 l/min into ICP-MS. The sample gas (argon) with flow rate of 0.6 l/min is admixed to the carrier gas flow after ablation cell. The ICP-MS conditions (gas flow rates, sampling depth and electrostatic lenses voltages of the mass spectrometer) were optimized in order to maximize signal/noise (S/N)

ratio and to achieve counts ratios of  $\text{ThO}^+/\text{Th}^+$  and  $\text{U}^+/\text{Th}^+$  lower than 0.2 and 1.1 %, respectively. All LA-ICP-MS measurements were done in single hole drilling mode with laser spot diameter of 40  $\mu\text{m}$ , laser fluence of 10  $\text{J/cm}^2$  and repetition rate of 10 Hz. For quantification purpose the certified reference material NIST SRM 612 was used. All measurements were normalized to average Ca concentration in triplite (8 638 ppm) and arrojadite-group minerals (14,598 ppm) measured by the electron microprobe.

## 4. Results

### 4.1. Fluorapatite

Fluorapatite is the most common phosphate in quartz veins. It forms green-grey, subhedral to anhedral grains (Fig. 2a) and aggregates up to 1.5 cm in size, which are enclosed in quartz, and frequently replaced by triplite (Fig. 2b). Rare are well developed, bluish-green prismatic fluorapatite crystals up to 2 mm in drusy cavities. Fluorapatite is homogenous in back-scattered electrons (BSE) mode (Fig. 2b); it shows  $\sim 1 \text{ apfu}$  F, distinct enrichment in Mn (around 0.3  $\text{apfu}$ , 3.8 to 4.3 wt. %  $\text{MnO}$ ) and low Fe content ( $\sim 0.03 \text{ apfu}$ , 0.3 to 0.5 wt. %  $\text{FeO}$ ).

### 4.2. Triplite

This mineral forms salmon-pink to red-brown subhedral to anhedral grains, up to 3.5 cm (Fig. 2a) or irregular aggregates up to 7 cm, which are embedded in massive quartz together with fluorapatite, minerals of arrojadite group, Fe-rich rhodochrosite, muscovite, arsenopyrite and Bi sulfosalts. Triplite is homogenous in BSE and it often replaces older aggregates of fluorapatite (Fig. 2b).

Triplite was confirmed by the P-XRD and its refined unit-cell parameters (Tab. 1) agree well with the published data and confirm the (1b) structure observed

**Tab. 3** LA-ICP-MS concentrations of elements in triplite (Trp) and arrojadite-group minerals (Arr) from Gemerská Poloma (in ppm)

Mineral	Trp	det. lim.								
Anal. #	1	2	3	4	5	6	7	8	9	
Li	8	7	7	4	7	9	8	13	13	2.9
Be	<	<	<	<	<	<	<	<	<	1.7
B	<	<	<	<	<	<	<	<	<	15
Na	<	<	<	<	155	<	<	158	<	145
Mg	2766	2723	1489	1455	2195	1719	2119	2330	2429	1.1
Al	25	3	12	14	4	4	<	8	3	1.6
Si	426	<	<	<	<	<	<	<	<	280
K	<	<	<	<	<	<	<	<	<	59
Sc	145	132	109	115	116	294	218	246	181	1
Ti	190	189	100	145	173	499	321	428	255	3
V	<	<	<	<	<	<	<	<	<	0.1
Cr	<	<	<	<	<	<	<	<	<	1.4
Co	<	<	<	<	<	<	<	<	<	0.1
Ni	<	<	<	<	<	<	<	<	<	2.6
Cu	<	<	<	<	<	<	<	<	<	0.8
Zn	359	330	236	231	309	379	314	470	356	0.1
Ga	<	<	<	<	<	<	<	<	<	0.1
Ge	<	<	<	<	<	<	<	<	<	2.9
As	<	<	<	<	<	<	<	<	<	2.9
Rb	1.7	1.4	1.5	2.0	2.2	<	<	1.5	1.6	1.1
Sr	4.8	1.8	37	47	1.4	0.7	0.9	1.0	1.0	0.1
Y	3.2	2.8	2.0	1.9	2.1	1.4	2.6	2.8	2.6	0.1
Zr	0.1	<	<	<	0.2	0.3	<	0.6	<	0.1
Nb	5.1	3.6	3.5	7.1	3.7	18.4	8.9	24	9.8	0.1
Sn	17	14	9.2	6.5	8.9	6.4	8.3	13	14	2.9
Sb	1.2	0.5	0.6	0.7	0.7	0.4	0.1	1.0	0.5	0.1
Ba	2.2	2.0	5.6	10	1.7	1.1	0.4	<	0.3	0.1
La	<	<	<	<	<	<	<	<	<	0.1
Ce	<	<	<	<	<	<	<	<	<	0.1
Pr	<	<	<	<	<	<	<	<	<	0.1
Nd	<	<	<	<	<	<	<	<	<	0.1
Sm	<	0.2	0.1	<	<	0.2	<	0.4	<	0.1
Eu	<	<	<	<	<	<	<	<	0.5	0.1
Gd	0.3	0.4	0.2	0.3	<	<	<	0.3	<	0.1
Tb	0.1	<	<	<	<	<	0.1	<	<	0.1
Dy	0.5	0.1	0.3	0.1	0.2	0.2	<	0.4	0.4	0.1
Ho	<	<	<	<	<	<	<	<	<	0.1
Er	0.2	0.3	0.2	0.2	0.1	<	0.2	0.3	<	0.1
Tm	<	<	<	<	<	<	<	<	<	0.1
Yb	0.5	0.3	0.1	0.4	<	0.3	0.5	0.7	0.8	0.1
Lu	<	0.1	<	<	<	<	<	<	<	0.1
Hf	<	<	<	<	<	<	<	<	<	0.1
Ta	0.2	0.1	0.2	0.4	<	3.0	1.4	5.5	0.9	0.1
Pb	<	<	0.8	0.6	0.6	0.6	<	<	<	0.1
Th	0.2	0.1	<	0.1	0.1	<	0.2	0.1	<	0.1
U	2.1	0.8	2.7	5.4	0.3	1.3	0.4	3.5	1.0	0.1

< = below detection limit (det. lim.)

for F-rich poor-Mg members of the wagnerite group (Lazic et al 2014). According to electron-microprobe measurements, triplite Mn/(Mn + Fe) atomic ratio attains 0.68–0.78 and F/(F + OH) ratio 0.89–0.92 (Tab. 2; Fig. 3a). Concentrations of Mg are negligible (around

**Tab. 3** LA-ICP-MS concentrations of elements in triplite (Trp) and arrojadite-group minerals (Arr) from Gemerská Poloma (in ppm) (continued)

Mineral	Arr									
Anal. #	1	2	3	4	5	6	7	8	9	10
Li	1330	1394	1248	1281	1318	1426	1290	1112	1330	1117
Be	3.9	3.9	3.7	4.4	2.3	3.1	3.7	3.2	3.9	3.8
B	16	<	<	<	<	<	<	<	<	<
Na	33826	34843	32288	34512	34558	32079	31463	35304	36088	30321
Mg	539	542	515	590	504	589	567	583	555	545
Al	10333	9817	9912	10725	9826	10766	11013	10934	10749	10177
Si	360	501	<	<	<	<	<	<	<	<
K	7158	7200	6937	7174	7200	7028	6409	6637	7612	6783
Sc	1028	973	885	1023	955	1167	973	1068	1028	979
Ti	188	196	177	196	196	132	164	163	219	181
V	<	<	<	<	<	<	<	<	<	<
Cr	<	<	<	<	<	<	<	<	<	<
Co	0.1	<	0.2	0.2	0.1	0.2	0.2	3.0	0.3	0.4
Ni	<	<	<	<	<	<	<	<	<	<
Cu	1.5	1.0	1.7	1.3	1.0	2.3	1.4	3.1	1.6	1.4
Zn	1813	1967	1861	1960	1792	1907	1790	1981	1685	1737
Ga	343	326	330	367	329	431	421	450	361	335
Ge	<	<	<	<	<	<	<	<	<	<
As	<	2.9	<	<	3.0	<	<	<	<	<
Rb	77	98	70	87	81	69	68	73	81	84
Sr	10141	9763	10216	11337	10942	9371	8898	9304	9159	10725
Y	20	21	19	25	20	19	17	19	28	25
Zr	0.8	0.8	0.9	0.9	0.7	0.5	0.7	0.7	0.8	0.7
Nb	0.3	0.2	0.3	0.4	0.6	0.4	0.3	0.3	0.4	0.2
Sn	11	9.7	8.0	11	7.0	7.4	8.0	8.3	11.2	8.8
Sb	0.2	<	0.1	<	0.4	0.1	0.2	<	0.3	0.2
Ba	20686	20705	21574	21384	20336	25053	24797	26739	22139	19478
La	2.9	2.9	2.7	3.2	2.6	2.6	2.4	2.5	3.3	3.1
Ce	4.6	4.7	4.3	5.2	5.1	4.3	4.5	4.1	7.2	6.4
Pr	0.5	0.4	0.4	0.5	0.6	0.4	0.4	0.6	0.6	0.7
Nd	1.3	1.2	1.2	1.5	1.7	1.0	1.5	1.0	2.4	2.2
Sm	0.5	0.8	0.7	0.5	0.8	0.4	0.7	0.6	0.7	1.2
Eu	0.5	0.7	0.6	0.6	0.6	0.9	0.8	1.0	0.8	0.5
Gd	0.4	0.5	0.5	0.2	0.8	0.9	0.9	0.8	1.4	0.8
Tb	0.2	0.3	0.3	0.3	0.2	0.4	0.2	0.3	0.3	0.3
Dy	2.1	2.4	2.0	1.7	2.6	1.9	2.0	2.3	2.9	2.9
Ho	0.6	0.6	0.4	0.6	0.5	0.4	0.5	0.5	0.7	0.5
Er	1.9	2.3	1.8	2.6	2.7	1.5	1.9	2.2	3.0	2.7
Tm	0.7	0.6	0.6	0.8	0.5	0.7	0.4	0.6	0.9	0.7
Yb	6.6	9.2	7.8	10.2	8.7	7.2	7.8	6.1	9.8	9.8
Lu	1.3	1.5	1.2	1.5	1.3	1.3	1.2	1.3	1.4	1.6
Hf	<	<	<	<	0	<	<	0	<	<
Ta	<	<	<	<	0	<	<	<	<	<
Pb	3309	3267	3127	3552	3424	2694	2565	2734	2984	3249
Th	0.2	0.1	0.2	0.2	0.1	0.1	0.2	0.2	0.1	0.2
U	1.3	1.2	1.3	1.6	0.8	1.1	1.4	2.2	1.6	2.3

0.02 apfu). The mineral contains 58–70 mol. % triplite, 19–27 mol. % zwieselite, 6–7 mol. % triploidite and 2–3 mol. % wolfeite end-member components; the concentrations of other molecules are under 2 mol. % (Tab. 2). Compositional variations of triplite indicate homovalent

substitutions between divalent cations:  $\text{FeMn}_{-1}$ ,  $\text{MgFe}_{-1}$ ,  $\text{MgMn}_{-1}$  and  $\text{CaMn}_{-1}$  (Fig. 3b–e).

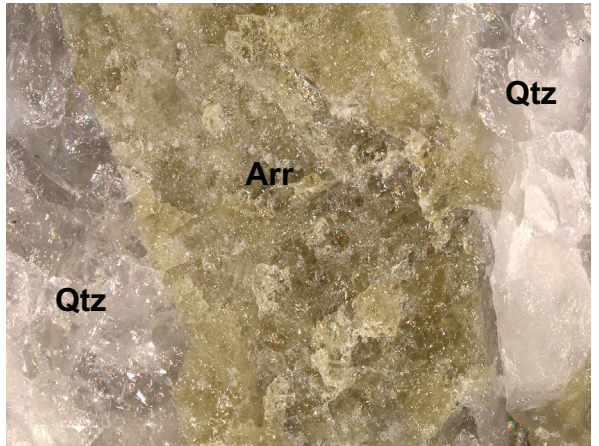
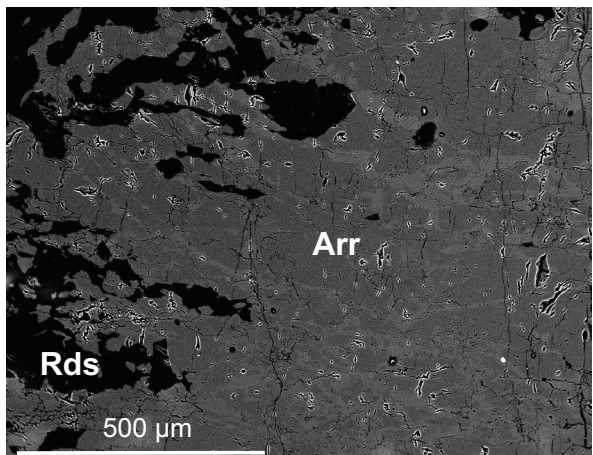
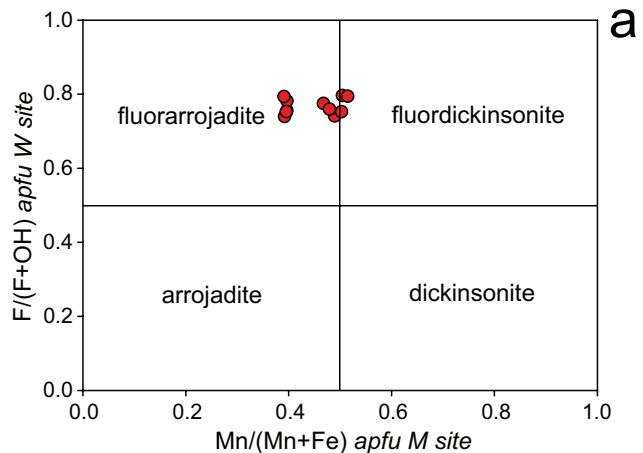
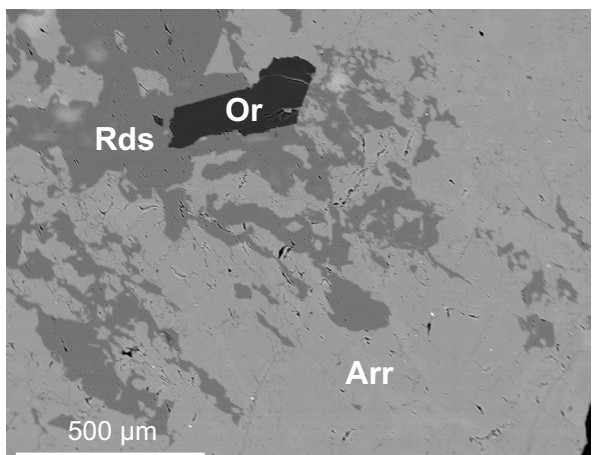
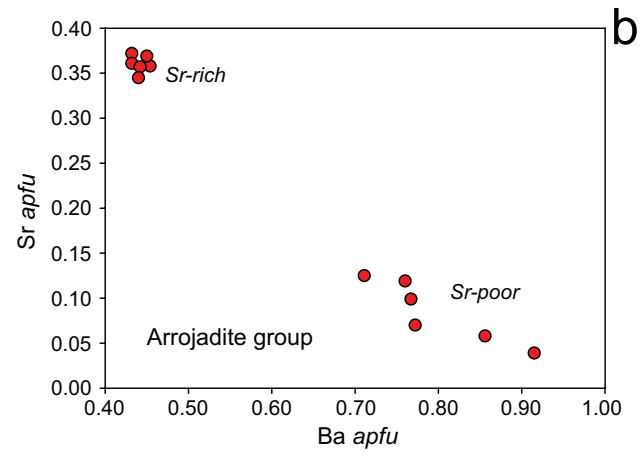
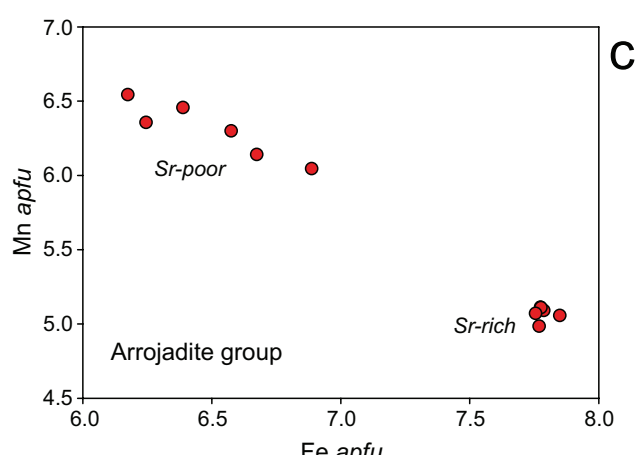
As shown by LA-ICP-MS analyses, triplite contains relatively low concentrations of trace elements: ~110 to 300 ppm Sc, 100 to 500 ppm Ti and 230 to 470 ppm Zn; concentrations of other measured trace elements are lower than 20 ppm (Tab. 3).

#### 4.3. "Fluorarrojadite-(BaNa)" to "fluordickinsonite-(BaNa)"

Minerals of arrojadite group occur as greenish-yellow to yellowish-brown anhedral grains and aggregates up to 2 cm in quartz veins (Fig. 4a), associated with fluorapatite, triplite, bismuthinite, kobellite and arsenopyrite. They are only slightly inhomogeneous in BSE (Fig. 4b), where the lighter zones are Ba-enriched. In some cases, they contain irregular microscopic aggregates of viitaniemiite and Fe-rich rhodochrosite. Graphic-like intergrowths of arrojadite group minerals and rhodochrosite were also observed (Fig. 4c).

The P-XRD data (Tab. 4) as well as refined unit-cell parameters of arrojadite-group minerals from the Gemerská Poloma are consistent with those reported from other localities (Tab. 5). Minerals of the arrojadite group have a very complex crystal chemistry and generalised formula of  $A_2B_2\text{CaNa}_{2+x}M_{13}\text{Al}(\text{PO}_4)_{11}(\text{PO}_3\text{OH})W_2$ , where  $A$  ( $A1$  and  $A2$ ) sites are occupied by either large divalent cations like  $\text{Ba}^{2+}$ ,  $\text{Sr}^{2+}$ ,  $\text{Pb}^{2+}$  and vacancy, or monovalent ( $\text{K}^+$ ,  $\text{Na}^+$ ) cations;  $B$  site ( $B1$  and  $B2$ ) is occupied by smaller divalent cations like  $\text{Fe}^{2+}$ ,  $\text{Mn}^{2+}$ ,  $\text{Mg}^{2+}$  and vacancy or by monovalent cation ( $\text{Na}^+$ ). Octahedrally coordinated  $M$  site can be occupied by dominant  $\text{Fe}^{2+}$  (arrojadite series),  $\text{Mn}^{2+}$  (dick-

insonite series), or  $\text{Mg}^{2+}$ ,  $\text{Zn}^{2+}$  and  $\text{Li}^+$ , whereas the  $W$  site represents monovalent anions:  $(\text{OH})^-$  or  $\text{F}^-$  (Cámarra et al. 2006; Chopin et al. 2006; Della Ventura et al. 2014). Based on electron-microprobe study, the studied arrojadite-group minerals belong to "fluorar-

**a****b****c**

**Fig. 4** Arrojadite-group minerals from Gemerská Poloma. **a** – olive green to yellowish-brown aggregate of “fluorarrojadite-(BaNa)” to “fluordickinsonite-(BaNa)” (Arr) enclosed in quartz (Qtz), width of image: 12 mm; **b** – Slightly irregular chemical zoning of arrojadite-group minerals (Arr) with rhodochrosite (Rds), BSE image; **c** – Graphic-like intergrowths of arrojadite-group minerals (Arr) with rhodochrosite (Rds) and minor orthoclase (Or), BSE image.

rojadite-(BaNa)” and its Mn-dominant analogue “fluordickinsonite-(BaNa)”. These are both IMA-CNMNC unapproved members of arrojadite group, according to the nomenclature of Chopin et al. (2006) (Tab. 6,

**Fig. 5** Classification and substitution diagrams of the arrojadite-group minerals from Gemerská Poloma. **a** – Quadrilateral Mn/(Mn + Fe) vs. W site F/(F + OH); **b** – Ba vs. Sr; **c** – Fe vs. Mn.

Fig. 5a). Our compositions are fluorine-dominant [W site F/(F + OH) = 0.74–0.80] and Fe-rich [Mn/(Mn + Fe) = 0.39–0.52], with high Ba and Na contents (3.0 to 6.3 wt. % BaO, 0.43–0.92 apfu Ba and ~5.5 wt. % Na<sub>2</sub>O, ~3.9 apfu Na). According to Ba/(Ba + Sr) atomic ratio, two compositional types could be recognized: Sr-rich “fluorarrojadite-(BaNa)” with ~1.7 wt.% SrO

**Tab. 4** Powder X-ray diffraction pattern of arrojadite-group minerals from Gemerská Poloma

<i>h</i>	<i>k</i>	<i>l</i>	<i>d</i> <sub>obs</sub>	<i>I</i> <sub>obs</sub>	<i>d</i> <sub>calc</sub>	<i>h</i>	<i>k</i>	<i>l</i>	<i>d</i> <sub>obs</sub>	<i>I</i> <sub>obs</sub>	<i>d</i> <sub>calc</sub>
2	0	2	7.586	4	7.618	5	1	9	2.3030	1	2.3031
1	1	2	7.361	2	7.419	5	3	5	2.2549	5	2.2510
2	0	2	5.908	8	5.905	3	3	8	2.2107	2	2.2103
2	0	4	5.487	7	5.519	7	1	6	2.1961	9	2.1929
1	1	4	5.211	5	5.225	0	2	10	2.1459	18	2.1441
0	2	0	4.997	5	5.010	4	4	3	2.1240	6	2.1243
3	1	2	4.749	6	4.760	4	4	0	2.1201	7	2.1186
3	1	0	4.683	7	4.682	4	4	4	2.0923	1	2.0928
0	2	2	4.604	21	4.615	2	0	12	2.0533	2	2.0525
1	1	4	4.554	18	4.561	3	3	7	2.0290	2	2.0309
2	0	4	4.235	3	4.236	2	4	6	1.9736	6	1.9750
2	2	2	4.181	6	4.186	2	4	8	1.9409	3	1.9387
3	1	2	4.046	2	4.038	7	3	4	1.9158	8	1.9169
0	2	4	3.824	7	3.827	3	1	13	1.8564	10	1.8567
0	2	5	3.445	7	3.445	1	3	11	1.8483	5	1.8478
1	1	6	3.402	47	3.400	7	1	5	1.8300	1	1.8299
1	1	7	3.320	26	3.315	8	2	1	1.8043	1	1.8058
2	2	4	3.240	9	3.235	5	1	13	1.7791	2	1.7782
1	3	1	3.217	49	3.214	8	2	2	1.7577	23	1.7583
1	3	2	3.197	8	3.197	4	2	13	1.7427	4	1.7432
4	2	0	3.115	10	3.112	6	2	12	1.7274	5	1.7270
5	1	4	3.033	100	3.031	3	3	10	1.6996	3	1.7002
0	0	8	2.965	7	2.965	3	1	12	1.6809	3	1.6830
1	3	4	2.932	5	2.932	9	1	2	1.6579	10	1.6580
4	2	2	2.873	6	2.856	6	4	4	1.6556	8	1.6556
3	3	2	2.846	18	2.842	2	6	2	1.6301	2	1.6311
3	1	8	2.826	16	2.829	3	1	15	1.6208	1	1.6201
5	1	6	2.772	4	2.773	5	5	7	1.6119	6	1.6115
3	3	1	2.757	40	2.759	6	4	10	1.5941	2	1.5935
4	2	3	2.709	83	2.708	3	5	7	1.5769	3	1.5775
3	3	2	2.669	5	2.663	9	1	4	1.5601	5	1.5601
5	1	3	2.613	2	2.613	9	3	1	1.5330	3	1.5335
1	3	6	2.592	7	2.591	4	6	1	1.5255	2	1.5258
0	2	8	2.553	35	2.552	9	3	2	1.5012	2	1.5016
0	4	0	2.507	27	2.505	3	5	11	1.4857	4	1.4866
5	1	8	2.4599	2	2.4583	9	1	13	1.4687	2	1.4685
4	2	8	2.4167	13	2.4171	7	5	2	1.4580	3	1.4581
4	2	5	2.3832	7	2.3817	3	3	13	1.4411	3	1.4412
3	1	10	2.3533	2	2.3546	5	5	11	1.4371	2	1.4368
5	3	1	2.3349	2	2.3355						

(~0.36 *apfu* Sr), and Sr-poor “fluorarrojadite-(BaNa)” to “fluordickinsonite-(BaNa)” with 0.2 to 0.6 wt.% SrO (0.04 to 0.13 *apfu* Sr). The corresponding Ba/(Ba +

Sr) ratios attain 0.54–0.56 and 0.85–0.96, respectively (Tab. 6, Fig. 5b). Potassium shows higher concentration in the Sr-rich compositions (0.9 to 1.0 wt. % K<sub>2</sub>O, 0.40–0.45 *apfu* K) in comparison with the Sr-poor analyses (0.6 to 0.8 wt. % K<sub>2</sub>O, 0.29–0.38 *apfu* K). Aluminum in the both types attains 0.98 to 1.05 *apfu*, totals of *M* site cations (Fe, Mn, Mg, Zn, Li) achieve 13.1 to 13.5. Average lithium content measured by LA-ICP-MS (1285 ppm Li, 0.28 wt. % Li<sub>2</sub>O, 0.41 *apfu*) is usually lower than theoretical Li contents (0.41–0.62 *apfu*) calculated according to Chopin et al. (2006), possibly due to uncertainty of measured Si and Al contents. Contents of Ti, Mg, and Zn are low ( $\leq 0.1$  *apfu*); other measured elements (S, As, Si, Cl) are below the respective detection limits of the electron microprobe. The compositional variations indicate the following substitution mechanisms which also differ between the Sr-rich and Sr-poor compositions: FeMn<sub>-1</sub> in *M* site (Fig. 5c), BaSr<sub>-1</sub> in *Al*+*Ca* sites (Fig. 5b), and F(OH)<sub>-1</sub> in *W* site (Tab. 6).

The LA-ICP-MS analyses of “fluorarrojadite-(BaNa)” to “fluordickinsonite-(BaNa)” reveal elevated concentrations of some elements: ~1100 to 1400 ppm Li, 2600 to 3600 ppm Pb,

1700 to 2000 ppm Zn, 900 to 1200 ppm Sc, 330 to 450 ppm Ga, 70 to 100 ppm Rb, and 17 to 28 ppm Y; concentrations of other trace elements are less than 20 ppm (Tab. 3).

#### 4.4. Viitaniemiite

Viitaniemiite Na(Ca,Mn)Al(PO<sub>4</sub>)F<sub>2</sub>(OH) is rarest phosphate in the studied association. It occurs as irregular grains and aggregates up to 150 µm in size (Fig. 6a), which are enclosed in arrojadite-group minerals together with Fe-rich rhodochrosite. Chemical composition of viitaniemiite (Tab. 7) shows a distinct enrichment in

**Tab. 5** Refined unit-cell parameters of arrojadite-group minerals from Gemerská Poloma in comparison with published data

	this work	Chopin et al. (2006)*
<i>a</i> [Å]	16.498(3)	16.4970(9)
<i>b</i> [Å]	10.019(2)	10.0176(5)
<i>c</i> [Å]	24.637(5)	24.6359(13)
$\beta$ [°]	105.65(2)	105.649(2)
<i>V</i> [Å <sup>3</sup> ]	3921(1)	3920.42(5)

\* data for fluorarrojadite-(BaFe)

**Tab. 6** Chemical composition of arrojadite-group minerals from Gemerská Poloma (in wt. %)

Anal. #	17	18	20	23	30	31	33	Average
Prefix	Fluor	Fluor	Fluor	Fluor	Fluor	Fluor	Fluor	Fluor
Root name	arrojadite	arrojadite	arrojadite	arrojadite	arrojadite	dickinsonite	dickinsonite	arrojadite
1 <sup>st</sup> suffix	Ba	Ba	Ba	Ba	Ba	Ba	Ba	Ba
2 <sup>nd</sup> suffix	Na	Na	Na	Na	Na	Na	Na	Na
P <sub>2</sub> O <sub>5</sub> EMPA-WDS	40.31	40.45	40.36	40.14	40.13	40.01	39.84	40.39
P <sub>2</sub> O <sub>5</sub> calc.	38.82	38.98	39.10	38.76	39.03	38.71	38.36	38.88
TiO <sub>2</sub>	0.05	0.06	0.05	0.06	0.06	0.09	0.04	0.06
Al <sub>2</sub> O <sub>3</sub>	2.28	2.39	2.44	2.38	2.44	2.40	2.41	2.39
FeO	25.50	25.57	25.89	22.52	21.56	20.86	19.98	23.41
MnO	16.46	16.59	16.47	19.52	20.48	20.82	20.91	18.41
ZnO	0.29	0.19	0.20	0.11	0.21	0.13	0.24	0.19
MgO	0.11	0.10	0.12	0.15	0.13	0.11	0.12	0.13
CaO	2.06	2.04	2.03	1.92	1.91	1.92	2.08	2.07
SrO	1.69	1.71	1.70	0.59	0.47	0.56	0.18	1.06
BaO	3.17	3.03	3.11	4.96	5.39	5.30	6.32	4.33
Li <sub>2</sub> O LA-ICP-MS	0.28	0.28	0.28	0.28	0.28	0.28	0.28	0.28
Na <sub>2</sub> O	5.48	5.48	5.37	5.36	5.41	5.44	5.36	5.46
K <sub>2</sub> O	0.96	0.94	0.89	0.82	0.78	0.81	0.63	0.84
H <sub>2</sub> O calc.	0.62	0.59	0.63	0.59	0.63	0.61	0.57	0.60
F	1.30	1.36	1.29	1.34	1.29	1.30	1.36	1.33
O=F	-0.55	-0.57	-0.54	-0.56	-0.54	-0.55	-0.57	-0.56
Total	98.52	98.74	99.03	98.80	99.62	98.79	98.27	98.88
P <sup>5+</sup>	12.000	12.000	12.000	12.000	12.000	12.000	12.000	12.000
Ti <sup>4+</sup>	0.981	1.024	1.042	1.026	1.044	1.036	1.050	1.027
Al <sup>3+</sup>	0.014	0.016	0.014	0.016	0.016	0.025	0.011	0.016
Sum Al	0.995	1.040	1.056	1.042	1.060	1.061	1.061	1.043
Fe (Fe <sup>2+</sup> )	7.787	7.776	7.849	6.887	6.575	6.388	6.174	7.138
Mn <sup>2+</sup>	5.091	5.110	5.057	6.046	6.300	6.457	6.544	5.685
Zn <sup>2+</sup>	0.078	0.051	0.054	0.030	0.056	0.035	0.065	0.051
Mg <sup>2+</sup>	0.060	0.054	0.065	0.082	0.070	0.060	0.066	0.071
Li <sup>+</sup>	0.411	0.409	0.408	0.412	0.409	0.412	0.416	0.411
Sum M	13.427	13.400	13.433	13.457	13.410	13.352	13.265	13.356
Ca <sup>2+</sup>	0.806	0.795	0.788	0.752	0.743	0.753	0.823	0.809
Sr <sup>2+</sup>	0.358	0.361	0.357	0.125	0.099	0.119	0.039	0.224
Ba <sup>2+</sup>	0.454	0.432	0.442	0.711	0.767	0.760	0.915	0.619
Na <sup>+</sup>	3.879	3.863	3.774	3.800	3.809	3.862	3.840	3.859
K <sup>+</sup>	0.447	0.436	0.412	0.383	0.361	0.378	0.297	0.391
Sum X	5.944	5.887	5.773	5.771	5.779	5.872	5.914	5.902
Sum M+X	19.371	19.287	19.206	19.228	19.189	19.224	19.179	19.258
Li calc.	0.406	0.543	0.590	0.551	0.610	0.616	0.611	0.556
<sup>M</sup> Fe*	0.427	0.400	0.433	0.457	0.410	0.352	0.265	0.356
Sum X <sup>2+</sup>	1.618	1.588	1.587	1.588	1.609	1.632	1.777	1.652
Sum cat.	32.366	32.327	32.262	32.269	32.249	32.284	32.240	32.301
OH <sup>-</sup>	1.499	1.436	1.521	1.450	1.518	1.495	1.411	1.466
F <sup>-</sup>	1.501	1.564	1.479	1.550	1.482	1.505	1.589	1.534
O (O <sup>2-</sup> )	47.000	47.000	47.000	47.000	47.000	47.000	47.000	47.000
Sum of anions	50.000	50.000	50.000	50.000	50.000	50.000	50.000	50.000
F/(F+OH) W	0.751	0.782	0.740	0.775	0.741	0.753	0.795	0.767
Mn/(Mn+Fe)	0.395	0.397	0.392	0.467	0.489	0.503	0.515	0.443

X = A1 + A2 + B1 + B2 + Ca + Na cation sites; formulae based on P = 12 apfu and (OH+F) = 3 apfu

S, As, Si, and Cl contents are below detection limit

Mn (10 to 11 wt. % MnO, 0.34–0.38 apfu Mn) which shows a positive correlation with Fe concentrations (1.8

to 2.6 wt. % FeO, 0.06–0.09 apfu Fe), possibly due to (Fe,Mn,Mg)Ca<sub>1-x</sub> substitution (Fig. 6b–c).

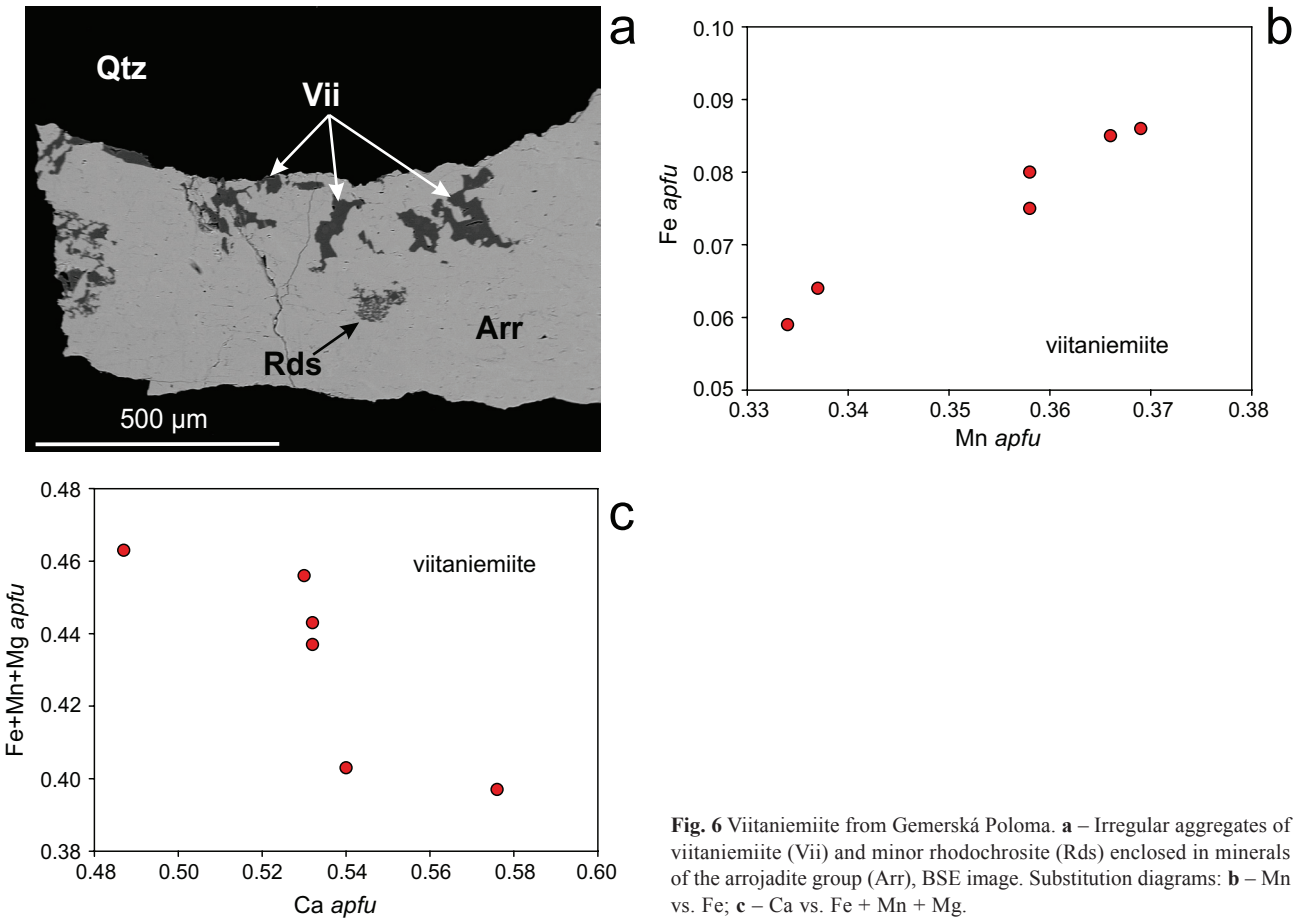


**Fig. 6** Viitaniemiite from Gemerská Poloma. **a** – Irregular aggregates of viitaniemiite (Vii) and minor rhodochrosite (Rds) enclosed in minerals of the arrojadite group (Arr), BSE image. Substitution diagrams: **b** – Mn vs. Fe; **c** – Ca vs. Fe + Mn + Mg.

## 5. Discussion and conclusions

The studied association represents F-rich, Mn, Fe, Ca-phosphate minerals which precipitated with massive quartz and minor Fe-rich rhodochrosite, albite, muscovite, fluorite and sulphide minerals. Fluorapatite is probably the oldest, as it is partly replaced by triplite (Fig. 2a–b). The mutual textural relationships between other phases are not unambiguous but indicate near contemporary origin of all the remaining phosphates together with quartz, rhodochrosite and other associated hydrothermal minerals. Such mineral assemblage as well as textural relationships indicates a relatively high-temperature, early hydrothermal (subsolidus) origin. Similar post-magmatic, early hydrothermal origin of triplite in granite-related quartz veins was proposed, for example, in Tigrinoe tin deposit, Russia (Gonevchuk et al. 2005), Huber stock near Horní Slavkov, Czech Republic (Sejkora et al. 2006), or Panasqueira, Portugal (Isaacs and Peacor 1981; Milá and Fabre 2014).

Both described members of arrojadite group [“fluorarrojadite-(BaNa)” and “fluordickinsonite-(BaNa)”] are still not officially approved as valid minerals by CNMNC IMA. However, “fluorarrojadite-(BaNa)” composition is documented from the Sidi-bou-Kricha pegmatite,

Morocco and it has been identified as a potential new mineral species (Chopin et al. 2006).

Unapproved fluor-dominant members of the arrojadite group [“fluorarrojadite-(BaNa)” and “fluorarrojadite-(SrNa)”] were also described from topaz-zinnwaldite microgranite of the Gemicic type from Surovec (Petrík et al. 2011), only ~8 km NNE of the locality studied here. “Fluordickinsonite-(BaNa)” compositions were also noted from the Surovec microgranite (Petrík et al. 2011) but the published crystallochemical formulae of the two analyses showed  $\text{Fe} > \text{Mn}$  and  $\text{Mn}/(\text{Mn} + \text{Fe}) < 0.5$  (0.48) in the  $M$  site; therefore they could be classified as “fluorarrojadite-(BaNa)” and “fluorarrojadite-(SrNa)”.

Viitaniemiite represents a rare Na–Ca–Al phosphate mineral, firstly described from granitic pegmatites in Eräjärvi area, Finland (Lahti 1981). Our compositions of viitaniemiite show a distinct Mn enrichment (10 to 11 wt. %  $\text{MnO}$ ) which is comparable with viitaniemiite from the Eräjärvi pegmatites (10–12 wt. %  $\text{MnO}$ ; Lahti 1981) and from the topaz-zinnwaldite microgranite in Surovec (8–10 wt. %  $\text{MnO}$ ; Petrík et al. 2011). On the other hand, viitaniemiite from alkali silicocarbonatites in Francon quarry, Montréal, Canada does not contain any detectable Mn (Ramik et al. 1983).

Experimental results indicate a relatively high solubility of P-rich and F-bearing magmatic liquids in aqueous fluids and subsequent precipitation of fluorite, topaz, apatite, and triplite in greisens, hydrothermal veins and miarolitic cavities associated with the P-rich granites (Webster et al. 1998). The Fe–Mn phosphate minerals (childrenite–eosphophite, zwiesselite and triphylite) were formed also during late-magmatic crystallization of the strongly P- and F-enriched residual melt in extremely fractionated, P-rich granite at Podlesí, Czech Republic (Breiter et al. 1997, 2005). Moreover, primary magmatic P-rich alkali feldspars (especially orthoclase) could be an alternative source of phosphorus (London 1992; Frýda and Breiter 1995), released during their post-magmatic alteration by F-rich fluids. This process would enable crystallization of early hydrothermal Fe-rich phosphates (Breiter et al. 1997) or fluorapatite (Broska et al. 2004).

Consequently, in the case of Gemerská Poloma we suggest a precipitation of the phosphates and associated minerals from alkali-, P- and F-rich post-magmatic to early hydrothermal, relatively high-temperature fluids which altered primary magmatic minerals (especially Li-rich micas and alkali feldspars) and liberated some elements (Fe, Mn, Al, Ca, Ba, Sr, Na and K) from the adjacent granite.

**Acknowledgements.** We would like to acknowledge Radek Škoda (Masaryk University, Brno), Peter Bačík (Comenius University, Bratislava) and Pavel Škácha (Mining Museum, Příbram) for their support of this study. Both referees, Fernando Câmara and Igor Petrík, same as handling editor Igor Broska and the editor-in-chief Vojtěch Janoušek, are highly acknowledged for comments and suggestions that helped to improve the manuscript. This work was financially supported by the Ministry of Culture of the Czech Republic (DKRVO 2015/02; National Museum 00023272).

**Tab. 7** Chemical composition of viitaniemiite from Gemerská Poloma (in wt. %)

Anal. #	22	24	25	26	27	28
P <sub>2</sub> O <sub>5</sub>	29.01	29.35	30.00	29.99	29.64	29.37
Al <sub>2</sub> O <sub>3</sub>	20.74	20.57	20.54	20.37	20.58	20.76
FeO	2.50	2.24	1.94	2.62	1.78	2.37
MnO	10.61	10.49	10.11	11.06	9.89	10.52
MgO	0.09	0.07	0.04	0.13	0.06	0.09
CaO	12.16	12.33	12.80	11.53	13.48	12.35
Na <sub>2</sub> O	12.67	12.74	12.70	12.15	12.26	12.80
H <sub>2</sub> O*	3.46	3.60	3.78	3.61	3.60	3.49
F	16.00	15.97	16.12	16.46	16.20	16.22
O=F	-6.74	-6.72	-6.79	-6.93	-6.82	-6.83
Total	100.50	100.64	101.24	100.99	100.67	101.14
P <sup>5+</sup>	1.000	1.000	1.000	1.000	1.000	1.000
Al <sup>3+</sup>	0.995	0.976	0.953	0.946	0.967	0.984
Fe <sup>2+</sup>	0.085	0.075	0.064	0.086	0.059	0.080
Mn <sup>2+</sup>	0.366	0.358	0.337	0.369	0.334	0.358
Mg <sup>2+</sup>	0.005	0.004	0.002	0.008	0.004	0.005
Ca <sup>2+</sup>	0.530	0.532	0.540	0.487	0.576	0.532
Sum M	0.986	0.969	0.943	0.950	0.973	0.975
Na <sup>+</sup>	1.000	0.994	0.970	0.928	0.947	0.998
OH <sup>-</sup>	0.940	0.967	0.993	0.950	0.958	0.937
F <sup>-</sup>	2.060	2.033	2.007	2.050	2.042	2.063
Sum X	3.000	3.000	3.000	3.000	3.000	3.000
O <sup>2-</sup>	3.980	3.930	3.857	3.831	3.896	3.951
Sum cat.	3.981	3.939	3.866	3.824	3.887	3.957
Sum an.	6.980	6.930	6.857	6.831	6.896	6.951
Mn/(Mn+Ca)	0.41	0.40	0.38	0.43	0.37	0.40

Formulae based on P = 1 apfu and (OH+F) = 3 apfu

S, As, Si, Ti, Zn, Sr, Ba, K, Cl were below detection limit

## References

- BAIJOT M, HATERT F, PHILIPPO S (2012) Mineralogy and geochemistry of phosphates and silicates in the Sapucaia pegmatite, Minas Gerais, Brazil: genetic implications. Canad Mineral 50: 1531–1554
- BAJANÍK Š, IVANIČKA J, MELLO J, PRISTAŠ J, REICHWALDER P, SNOPKO L, VOZÁR J, VOZÁROVÁ A (1984) Geological map of the Slovenské Rudohorie Mts.–eastern part 1 : 50 000. Dionýz Štúr Institute of Geology, Bratislava
- BREITER K, FRÝDA J, SELTMANN R, THOMAS R (1997) Mineralogical evidence for two magmatic stages in the evolution of an extremely fractionated P-rich rare-metal granite: the Podlesí stock, Krušné Hory, Czech Republic. J Petrol 38: 1723–1739
- BREITER K, MÜLLER A, LEICHMANN J, GABAŠOVÁ A (2005) Textural and chemical evolution of a fractionated granitic system: the Podlesí stock, Czech Republic. Lithos 80: 323–345
- BREITER K, BROSKA I, UHER P (2015) Intensive low-temperature tectono-hydrothermal overprint of peraluminous rare-metal granite: a case study from the Dlhá dolina Valley (Gemicicum, Slovakia). Geol Carpath 66: 19–36

- BROSKA I, WILLIAMS CT, UHER P, KONEČNÝ P, LEICHMANN J (2004) The geochemistry of phosphorus in different granite suites of the Western Carpathians, Slovakia: the role of apatite and P-bearing feldspar. *Chem Geol* 205: 1–15
- CÁMARA F, OBERTI R, CHOPIN C, MEDENBACH O (2006) The arrojadite enigma: I. A new formula and a new model for the arrojadite structure. *Amer Miner* 91: 1249–1259
- CHOPIN C, OBERTI R, CÁMARA F (2006) The arrojadite enigma: II. Compositional space, new members, and nomenclature of the group. *Amer Miner* 91: 1260–1270
- DELLA VENTURA G, BELLATRECCIA F, RADICA F, CHOPIN C, OBERTI R (2014) The arrojadite enigma III. The incorporation of volatiles: a polarised FTIR spectroscopy study. *Eur J Mineral* 26: 679–688
- DIANIŠKA I, BREITER K, BROSKA I, KUBIŠ M, MALACHOVSKÝ P (2002) First phosphorous-rich Nb-Ta-Sn-specialised granite from the Carpathians – Dlhá dolina Valley granite pluton, Gemicic Superunit. *Geol Carpath* 53: Special Issue (CD-ROM).
- DIANIŠKA I, UHER P, HURAI V, HURAIOVÁ M, FRANK W, KONEČNÝ P, KRÁL J (2007) Mineralization of rare-metal granites. In: HURAI V (ed) Sources of Fluids and Origin of Mineralizations in the Gemicic Unit. Open file report, Dionýz Štúr Institute of Geology, Bratislava, pp 254–330 (in Slovak)
- DOWNS RT (2006) The RRUFF Project: an integrated study of the chemistry, crystallography, Raman and infrared spectroscopy of minerals. Program and Abstracts of the 19<sup>th</sup> General Meeting of the International Mineralogical Association in Kobe, Japan, O03-13
- FRÝDA J, BREITER K (1995) Alkali feldspars as a main phosphorus reservoirs in rare-metal granites: three examples from the Bohemian Massif (Czech Republic). *Terra Nova* 7: 315–320
- GAAB AS, TODT W, POLLER U (2006) CLEO: Common lead evaluation using Octave. *Comput Geosci* 32: 993–1003
- GONEVCHUK VG, KOROSTELEV PG, SEMENYAK BI (2005) Genesis of the Tigrinoe tin deposit (Russia). *Geol Ore Deposits* 47: 223–237
- ISAACS AM, PEACOR DR (1981) Panasqueirite, a new mineral: The OH-equivalent of isokite. *Canad Mineral* 19: 389–392
- KILÍK J (1997) Geological characteristic of the talc deposit in Gemerská Poloma–Dlhá dolina. *Acta Montan Slovaca* 2: 71–80 (in Slovak)
- KOHÚT M, STEIN H (2005) Re–Os molybdenite dating of granite-related Sn–W–Mo mineralisation at Hnilec, Gemicic Superunit, Slovakia. *Miner Petrol* 85: 117–129
- KUBIŠ M, BROSKA I (2005) The role of boron and fluorine in evolved granitic rock systems (on the example of the Hnilec area, Western Carpathians). *Geol Carpath* 56: 193–204
- KUBIŠ M, BROSKA I (2010) The granite system near Betliar village (Gemicic Superunit, Western Carpathians): evolution of a composite silicic reservoir. *J Geosci* 55: 131–148
- LAHTI SI (1981) On the granitic pegmatites of the Eräjärvi area in Orivesi, southern Finland. *Geol Surv Finland Bull* 314: 1–82
- LAUGIER J, BOCHU B (2011) LMGP – Suite of Programs for the Interpretation of X-ray Experiments. Accessed on December 2, 2015, at <http://www.ccp14.ac.uk/tutorial/lmpg>
- LAZIC B, ARMBRUSTER T, CHOPIN C, GREW ES, BARONNET A, PALATINUS L (2014) Superspace description of wagnerite-group minerals  $(\text{Mg},\text{Fe},\text{Mn})_2(\text{PO}_4)(\text{F},\text{OH})$ . *Acta Cryst B* 70: 243–258
- LLORENS T, MORO MC (2012) Fe–Mn phosphate associations as indicators of the magmatic–hydrothermal and supergene evolution of the Jálama Batholith in the Navasfrías Sn–W District, Salamanca, Spain. *Mineral Mag* 76: 1–24
- LONDON D (1992) Phosphorus in S-type magmas: the  $\text{P}_2\text{O}_5$  content of feldspars from peraluminous granites, pegmatites and rhyolites. *Amer Miner* 77: 126–145
- LONDON D (1997) Estimating abundances of volatile and other mobile components in evolved silicic melts through mineral–melt equilibria. *J Petrol* 38: 1691–1706
- MILÁ CC, FABRE J (2014) The Panasqueira mines, Castelo Branco district, Portugal. *Mineral Rec* 45: 11–55
- PETRASOVÁ K, FARYAD SW, JEŘÁBEK P, ŽÁČKOVÁ E (2007) Origin and metamorphic evolution of magnesite–talc and adjacent rocks near Gemerská Poloma, Slovak Republic. *J Geosci* 52: 125–132
- PETRÍK I, KOHÚT M (1997) The evolution of granitoid magmatism during the Hercynian orogen in the Western Carpathians. In: GRECULA P, HOVORKA D, PUTIŠ M (eds) Geological Evolution of the Western Carpathians. Miner Slov, Monogr, 235–252
- PETRÍK I, KUBIŠ M, KONEČNÝ P, BROSKA I, MALACHOVSKÝ P (2011) Rare phosphates from the Surovec topaz–Li mica microgranite, Gemicic Unit, Western Carpathians, Slovak Republic: role of  $\text{F}/\text{H}_2\text{O}$  of the melt. *Canad Mineral* 49: 521–540
- PETRÍK I, ČÍK Š, MIGLIERINI M, VACULOVÍČ T, DIANIŠKA I, OZDÍN D (2014) Alpine oxidation of lithium micas in Permian S-type granites (Gemicic unit, Western Carpathians, Slovakia). *Mineral Mag* 78: 507–533
- PICCOLI PM, CANDELA PA (2002) Apatite in igneous systems. In: KOHN MJ, RAKOVAN J, HUGHES JM (eds) Phosphates: Geochemical, Geobiological, and Materials Importance. Mineralogical Society of America, Reviews in Mineralogy & Geochemistry 48, Washington, pp 256–292
- POUCHOU JL, PICHOIR F (1985) “PAP” ( $\text{ppZ}$ ) procedure for improved quantitative microanalysis. In: ARMSTRONG JT (ed) Microbeam Analysis. San Francisco Press, pp 104–106
- POLLER U, UHER P, BROSKA I, PLAŠIENKA D, JANÁK M (2002) First Permian–Early Triassic zircon ages for tin-bearing granites from the Gemicic Unit (Western Carpathians,

- Slovakia): connection to the post-collisional extension of the Variscan orogen and S-type granite magmatism. *Terra Nova* 14: 41–48
- RAMIK RA, STURMAN BD, ROBERTS AC, DUNN PJ (1983) Viitaniemiite from the Francon quarry, Montreal, Quebec. *Can Mineral* 21: 499–502
- RODA-ROBLES E, PESQUERA A, GIL-CRESPO P, TORRES-RUIZ J (2012) The Puentemocha beryl–phosphate granitic pegmatite, Salamanca, Spain: internal structure, petrography and mineralogy. *Canad Mineral* 50: 1573–1597
- SEJKORA J, ŠKODA R, ONDRUŠ P, BERAN P, SÜSSER C (2006) Mineralogy of phosphate accumulations in the Huber stock, Krásno ore district, Slavkovský les area, Czech Republic. *J Czech Geol Soc* 51: 103–147
- UHER P, BROSKA I (1996) Post-orogenic Permian granitic rocks in the Western Carpathian–Pannonian area: geochemistry, mineralogy and evolution. *Geol Carpath* 47: 311–321
- WALDROP L (1969) The crystal structure of triplite,  $(\text{Mn}, \text{Fe})_2\text{FPO}_4$ . *Z Kristallogr* 130: 1–14
- WEBSTER JD, THOMAS R, VEKSLER I, RHEDE D, SELTMANN R, FÖRSTER H-J (1998) Late-stage processes in P- or F-rich granitic magmas. *Acta Univ Carol, Geol* 42: 181–188